Journal of Molecular Spectroscopy 327 (2016) 21–30

Contents lists available at ScienceDirect

Journal of Molecular Spectroscopy

journal homepage: www.elsevier.com/locate/jms

Calculation of rotation-vibration energy levels of the ammonia molecule based on an *ab initio* potential energy surface

Oleg L. Polyansky [a,b,*], Roman I. Ovsyannikov [b], Aleksandra A. Kyuberis [b], Lorenzo Lodi [a], Jonathan Tennyson [a], Andrey Yachmenev [a], Sergei N. Yurchenko [a], Nikolai F. Zobov [b]

[a] *Department of Physics and Astronomy, University College London, Gower Street, London WC1E 6BT, United Kingdom*
[b] *Institute of Applied Physics, Russian Academy of Science, Ulyanov Street 46, Nizhny Novgorod 603950, Russia*

ARTICLE INFO

Article history:
Received 14 December 2015
In revised form 29 July 2016
Accepted 1 August 2016
Available online 9 August 2016

Keywords:
Ammonia
Global potential energy surface
Ab initio
Rovibrational levels
Dissociation energy

ABSTRACT

An *ab initio* potential energy surface (PES) for gas-phase ammonia NH_3 has been computed using the methodology pioneered for water (Polyansky et al., 2013). Multireference configuration interaction calculations are performed at about 50 000 points using the aug-cc-pCVQZ and aug-cc-pCV5Z basis sets and basis set extrapolation. Relativistic and adiabatic surfaces are also computed. The points are fitted to a suitable analytical form, producing the most accurate *ab initio* PES for this molecule available. The rotation-vibration energy levels are computed using nuclear motion program TROVE in both linearised and curvilinear coordinates. Better convergence is obtained using curvilinear coordinates. Our results are used to assign the visible spectrum of $^{14}NH_3$ recorded by Coy and Lehmann (1986). Rotation-vibration energy levels for the isotopologues NH_2D, NHD_2, ND_3 and $^{15}NH_3$ are also given. An *ab initio* value for the dissociation energy D_0 of $^{14}NH_3$ is also presented.

1. Introduction

Ammonia is a hazardous chemical, highly toxic for aquatic life, and its ever-increasing release into Earth's atmosphere has undesirable consequences [1]; monitoring its presence in the atmosphere is therefore a particularly important scientific objective. Remote sensing of spatially resolved atmospheric concentrations of ammonia requires reliable and extensive spectroscopic datasets and their deficiencies remain a significant source of error [2]. Another important area which requires spectroscopic data is astronomy; ammonia is thought to be the key spectroscopic signature of the coldest failed stars, so-called brown dwarfs [3,4], and is probably also prominent in the atmospheres of exoplanetary gas giants [5]. All these applications require accurate spectroscopic data over extended frequency and temperature ranges. Such data are also required for the analysis and assignment of hot laboratory spectra [6–9].

A review of experimental spectroscopic studies on $^{14}NH_3$ is given as part of a recent analysis [10], which provides the most extensive set of experimentally deduced energy levels for this system available to date. Unfortunately the available experimental data could only determine 30 vibrational band origins and only about 5000 rotation-vibrational (rovibrational) energy levels, so that any dataset which aims at completeness must rely on calculations; there is therefore a strong need for improved theoretical models of ammonia.

Very accurate *ab initio* calculations of the low-lying energy levels of NH_3 were performed by Rajamäki et al. [11,12] using coupled-clusted (CC) methods. It is well known, however, that CC methods experience difficulties for calculations of highly excited rovibrational energy levels. That is why the ability to calculate very accurately *ab initio* surfaces using multireference configuration interaction (MRCI) methods is important, as this can provide an accurate global surface which can give good results for both low-lying and highly excited vibrational energy levels. Recently two high-accuracy *ab initio* studies of the rotation-vibration energy levels of ammonia have been performed by Huang et al. [13–15] and by Yurchenko et al. [16–18] using high-quality, semi-empirical potential energy surfaces. In particular, Yurchenko et al. computed a linelist called BYTe including energy levels up to 18 000 cm^{-1}, containing over a billion transitions [17] and providing the most comprehensive spectral coverage for $^{14}NH_3$. The energy levels of BYTe, more accurate below 5000 cm^{-1}, already at 6000–7000 cm^{-1} differ from experiment by up to 5 cm^{-1}, so that this database is not always able to provide so-called spectroscopic accuracy (i.e., line positions accurate to better than 1 cm^{-1}) and

---

* Corresponding author at: Department of Physics and Astronomy, University College London, Gower Street, London WC1E 6BT, United Kingdom.

E-mail address: o.polyansky@ucl.ac.uk (O.L. Polyansky).

http://dx.doi.org/10.1016/j.jms.2016.08.003
0022-2852/© 2016 Elsevier Inc. All rights reserved.

consequently cannot address important unresolved issues such as the unassigned visible wavelength spectrum of $^{14}NH_3$ recorded by Coy and Lehmann three decades ago [19,20]. BYTe is also not appropriate for calculations of high-temperature spectra ($T > 1200$ K) as such studies require energy levels up to at least 20000 cm^{-1} [21]. All these considerations provide key motivations for constructing a new, more accurate and more extensive ammonia PES.

This paper is organised as follows. In Section 2 the *ab initio* method used is described, the choice of the grid points is given and the fitting procedure of these points to obtain analytical PES is presented. In Section 3 we present a new theoretical value for the dissociation energy D_0 of ammonia with an estimated uncertainty bar of ±35 cm^{-1}, which is much smaller than in all previous calculations; for example, in a recent study Marquardt et al. [22] report computed values for the dissociation energy with a scatter of about 1000 cm^{-1}. Out theoretical value for D_0 is in disagreement with the corresponding experimental value. In Section 4 we describe our nuclear motion calculations using the program TROVE [23,24] in both linearised and curvilinear coordinates. In Section 5 the results of the rotation-vibrational energy levels of ammonia NH_3 and its isotopologues are described and a comparison of these calculations with experimental data are presented; because of the much increased effort required for ammonia we could not afford the same level of *ab initio* theory used for water [25] but nevertheless we were still able to compute accurate energy levels up to 18000 cm^{-1}, covering all experimentally known levels. Section 6 concludes this paper.

2. Calculation of the *ab initio* PES

2.1. Electronic structure calculations

In the present study we apply an *ab initio* calculation scheme originally developed by us for the water molecule [25] and which was able to reproduce rovibrational energy levels of that molecule with a very high accuracy of about 0.1 cm^{-1}. The same approach has recently been applied, with very good results, to the molecular ion H_2F^+ [26]. Our calculation scheme comprises 11 components, is expected to lead to very accurate PESs and is applicable to small molecules made up by the atoms from the first and second periods of the periodic table (H to Ne). The various components are described in detail in Ref. [26] and we present them here only summarily: (1) a main component based on multi-reference configuration interaction (MRCI) [27] in the full-valence complete active space and the aug-cc-pCV6Z basis set [28–30]; (2) a basis set correction based on extrapolation [31–33] using the aug-cc-pCV5Z basis sets; (3) a dense grid of geometries [26,34–37]; (4) an electron correlation correction based on larger active spaces; (5) an adiabatic Born-Oppenheimer diagonal correction (BODC); (6) a scalar-relativistic correction [38,39]; (7) a higher-level relativistic correction based on the Dirac-Coulomb-Breit equation [40–42]; (8) a quantum electrodynamic correction (QED) [43–45]; (9) a non-adiabatic vibrational correction [25,46–48]; (10) a non-adiabatic rotational correction [47,49,50]; (11) an off-diagonal spin-orbit correction [51–53].

In the following we will use the abbreviations ac*n*z to indicate the aug-cc-pCV*n*Z basis sets and awc*n*z to indicate aug-cc-pwCV*n*Z ones [28–30].

The MRCI energies of points (1) and (4) should include size-extensivity corrections [27] (Davidson correction, +Q, or Pople correction) or size-extensivity-corrected MRCI-type schemes such as the Averaged Coupled Pair Functional (ACPF) [54] or the averaged quadratic coupled-cluster (AQCC) [55] methods can be used instead; however, our recommendation is to use MRCI+Q as other methods did not lead to better results in our tests with small molecules with up to five atoms. Internal contraction approximation schemes [56,57] may be used for MRCI.

At the moment it seems that, at least for the purposes of high-resolution spectroscopy of small molecules, the MRCI-type methods mentioned above provide the best possible accuracy; more advanced multi-reference coupled cluster approaches [58] have not yet been shown to produce superior results (see, e.g., table I of Ref. [59]).

Ammonia, like water and H_2F^+, is a ten-electron system but the presence of one more hydrogen atom renders it a substantially harder system from the point of view of *ab initio* calculations; the main reasons why this is so are: (i) the PES depends on 6 internal coordinates instead of only 3, therefore many more single-point calculations are needed to sample it. (ii) Each electronic-structure calculation is more expensive for ammonia than for water; in any given basis set the supplementary hydrogen atom increases the number of basis functions by about 30%, and as electronic-structure methods scale with the number of basis functions N at least as N^4 this modest increase in basis functions brings about a slowdown by a factor about 3 with respect to water; furthermore, in multi-reference methods such as CASSCF (complete active space self-consistent field) and MRCI [27] the size of the active space is also larger, resulting in a further significant slowdown for these methods. Finally, (iii) because of the larger dimensionality the nuclear-motion problem is much more difficult to treat; this added complexity manifests itself with a number of novel properties not present in triatomic molecules, such as the splitting of its energy levels due to the umbrella motion. This makes the spectra of ammonia hard to analyse [19,20,60,61].

We could not use all 11 components of our method in the present work for a variety of reasons. First of all tetratomic molecules requires about 50000 points, instead of about 2000 necessary for a triatomic calculation. Our computer resources did not allow us to calculate 50000 points using an aug-cc-pCV6Z basis set, so we had to limit ourselves to the aug-cc-pwCV5Z one. In addition, we only used first-order relativistic corrections, without Breit or Gaunt terms. The QED correction, which is needed to achieve 0.1 cm^{-1} accuracy, was not deemed necessary for the present aim of about 1 cm^{-1} accuracy and was not included either. Non-adiabatic corrections were allowed for by the primitive change of nuclear masses to atomic masses. Future work aimed at achieving 0.1 cm^{-1} accuracy will have to consider all these corrections.

In conclusion we computed a main surface using the aug-cc-pwCV5Z basis set and MRCI in the full-valence reference space, comprising 8 electrons in 7 orbitals. The MRCI calculations used the Celani-Werner internal contraction scheme [62,57] and took about 50 GB of disk space, 3 GB of RAM and 7 h of real time per geometry running on a single processor. A second surface computed with the same method but the smaller aug-cc-pwCVQZ basis set was computed in order to perform basis-set extrapolation of the energies; each of these took about 10 GB of disk space and 45 min of run time on the same system. An electronic correlation correction surface was computed with the aug-cc-pVQZ basis set and an extended reference space including two more orbitals; these calculations took about 1.5 h per geometry. For the relativistic correction we used the expectation value of the MVD1 operator for the CASSCF wave functions in the aug-cc-pwCV5Z basis set. Overall our calculations required about 270000 CPU-hours ($\approx$31 CPU-years).

2.2. Fit to an analytic form

In this study we used the grid of 51816 geometries from Ref. [63], which was designed to include all important geometries covering the energy region below 20 000 cm^{-1}. However, as discussed below, only 22 494 points were actually used in the final fit. To represent the *ab initio* data sets analytically we use a form which has already been used in a series publications to represent the PES not only of NH_3 [64] but also of other molecules and molecular ions PH_3, SbH_3, BeH_3, NH_3^+, CH_3^+, H_3O^+ [64–69].

$$\begin{aligned} V(\xi_1,\xi_2,\xi_3,\xi_{4a},\xi_{4b};\sin\bar{\rho}) = {} & V_\mathrm{e} + V_0(\sin\bar{\rho}) + \sum_j F_j(\sin\bar{\rho})\,\xi_j \\ & + \sum_{j\leqslant k} F_{jk}(\sin\bar{\rho})\,\xi_j\,\xi_k \\ & + \sum_{j\leqslant k\leqslant l} F_{jkl}(\sin\bar{\rho})\,\xi_j\,\xi_k\,\xi_l \\ & + \sum_{j\leqslant k\leqslant l\leqslant m} F_{jklm}(\sin\bar{\rho})\,\xi_j\,\xi_k\,\xi_l\,\xi_m \\ & + \sum_{j\leqslant k\leqslant l\leqslant m\leqslant n} F_{jklmn}(\sin\bar{\rho})\,\xi_j\,\xi_k\,\xi_l\,\xi_m\,\xi_n \\ & + \sum_{j\leqslant k\leqslant l\leqslant m\leqslant n\leqslant o} F_{jklmno}(\sin\bar{\rho})\,\xi_j\,\xi_k\,\xi_l\,\xi_m\,\xi_n\,\xi_o \end{aligned} \tag{1}$$

where

$$\xi_k = 1 - \exp(-a(r_k - r_\mathrm{e})), \quad k = 1,2,3, \tag{2}$$

$$\xi_{4a} = \frac{1}{\sqrt{6}}(2\alpha_1 - \alpha_2 - \alpha_3), \tag{3}$$

$$\xi_{4b} = \frac{1}{\sqrt{2}}(\alpha_2 - \alpha_3), \tag{4}$$

r_e denotes the equilibrium value of r_k, and

$$\sin\bar{\rho} = \frac{2}{\sqrt{3}}\sin[(\alpha_1 + \alpha_2 + \alpha_3)/6]. \tag{5}$$

The pure inversion potential energy function in Eq. (1) is given by

$$V_0(\sin\bar{\rho}) = \sum_{s=1}^{8} f_0^{(s)}\,(\sin\rho_e - \sin\bar{\rho})^s, \tag{6}$$

and the functions $F_{jk\ldots}(\sin\bar{\rho})$ are defined as

$$F_{jk\ldots}(\sin\bar{\rho}) = \sum_{s=0}^{N} f_{jk\ldots}^{(s)}\,(\sin\rho_e - \sin\bar{\rho})^s \tag{7}$$

where $\sin\rho_e$ is the equilibrium value of $\sin\bar{\rho}, a$ is a molecular parameter, and the quantities $f_0^{(s)}$ and $f_{jk\ldots}^{(s)}$ in Eqs. (6) and (7) are expansion coefficients. The summation limits in Eq. (7) are $N = 6$ for $F_j(\sin\bar{\rho}), N = 4$ for $F_{jk}(\sin\bar{\rho}), N = 3$ for $F_{jkl}(\sin\bar{\rho}), N = 2$ for $F_{jklm}(\sin\bar{\rho}), F_{jklmn}(\sin\bar{\rho})$, and $F_{jklmno}(\sin\bar{\rho})$. In total there are 301 symmetry unique potential parameters $f_{jk\ldots}^{(s)}$. The symmetry relations between the parameters can be found in, for example, Ref. [63].

The potential parameters $f_0^{(s)}$ and $f_{jk\ldots}^{(s)}$ were obtained by fitting to 22 494 *ab initio* energies; 301 parameters were used to reproduce all these energies with a fitting error of 3.2 cm^{-1}. The potential parameters together with a Fortran 90 program are given as supplementary material to this paper.

During fitting we assigned to each point an energy-dependent weight given by

$$w = \frac{2}{1 + e^{2\cdot 10^{-4}\cdot E}} \tag{8}$$

where E is the energy in cm^{-1}. The lowest point has zero energy and hence a weight equal to unity. Some of *ab initio* points showed unsatisfactory accuracy, for example due to issues with convergence in our *ab initio* calculations. Such points could be detected in the fitting procedure by a simple test: the fitted analytic PES lies far away from inaccurate points. The accuracy of the final PES is systematically increased by excluding inaccurate points from the fitting procedure.

In this work we fitted directly the sum of basis set extrapolated energies, relativistic corrections and higher-order correlation corrections; it was found beneficial to operate in this way as fitting the components separately resulted in larger fitting errors. The adiabatic correction was fitted separately as this made calculations for multiple isotopologues more convenient.

At the end of the initial 51 816 unique geometry points we used only 23 725 for the fit, as many points had to be excluded because at least one of the calculations (awc4z, awc5z, a4z/large cas) was missing (either because of numerical convergence problems or technical issues such as running out of disk space or allotted runtime).

3. Calculation of the dissociation energy

In our previous theoretical calculations [70] we were able to produce a theoretical value for the dissociation energy of water, D_0, with an estimated error of 8 cm^{-1} and in perfect agreement with the very accurate experimental value; in this section we compute an accurate value of the dissociation energy D_0 of ammonia, an important quantity in thermochemistry. The lowest dissociation pathway for ammonia consists in stretching to infinity one of the hydrogen atoms, and we define the dissociation energy D_0 as

$$D_0 = E_\mathrm{rvb}(NH_2) + E_\mathrm{rvb}(H) - E_\mathrm{rvb}(NH_3) \tag{9}$$

where the E_rvb are the total (rovibronic) ground state energies of NH_3 and of the dissociation fragments. In the Born-Oppenheimer approximation each rovibronic energy is written as a sum of an electronic energy E_el evaluated at the equilibrium geometry and of a ro-vibrational energy E_vib. As is customary we define the potential well depth D_e by an expression analogous to Eq. (9) but involving the electronic energies of the various fragments evaluated at their equilibrium (eq) geometries:

$$D_e = E_\mathrm{el}(NH_2,\mathrm{eq}) + E_\mathrm{el}(H,\mathrm{eq}) - E_\mathrm{el}(NH_3,\mathrm{eq}) \tag{10}$$

We also define the ro-vibrational zero-point energy (ZPE) of a system as the difference between the energy of the ro-vibrational ground state and the electronic energy evaluated at the equilibrium geometry. With these definitions we have that

$$D_0 = D_e + \mathrm{ZPE}(NH_2) + \mathrm{ZPE}(H) - \mathrm{ZPE}(NH_3) \tag{11}$$

Experimentally one of the first accurate values for D_0 was reported by Bohme et al. [71] as $D_0 = 106.0 \pm 1.1$ kcal/mol (37 074 ± 350 cm^{-1}); this value is in agreement with the later value by Gibson et al. [72] $D_0 = 106.7 \pm 0.3$ kcal/mol (37 300 ± 100 cm^{-1}), which is widely reported in the literature. Qi et al. [73] reported in 1995 a value $D_0 = 4.97 \pm 0.05$ eV (40 100 ± 400 cm^{-1}), considerably higher than previous values and in substantial disagreement with them. In 1996 Mordaunt et al. [74] reported very accurate values of the dissociation energies of five ammonia isotopologues, reporting for the parent isotopologue $^{14}NH_3$ $D_0 = 37\,115 \pm 20$ cm^{-1}, in agreement with the value of Bohme et al. and in mild disagreement (by 2σ) with the one of Gibson et al. Mordaunt et al. also report an experimentally-derived value for the potential well depth $D_e = 40\,510 \pm 25$ cm^{-1}. As discussed later in this section, our calculations lead to values for D_0 and D_e which are in substantial disagreement with experiment.

An *ab initio* value for D_e for ammonia was computed using high-order coupled cluster theory and Eq. (10); because only calculations at equilibrium geometries are required the coupled cluster hierarchy is expected to converge very quickly and therefore we

Table 1
Ab initio contributions to the dissociation energies of NH_3. All values are in cm^{-1}. Uncertainties are given in parenthesis. Signed contributions are additive corrections. Quantities A to F are nuclear-mass independent, all others are nuclear-mass dependent. See text for a full description of the contributions.

Label	Description	Value unc.
A	CCSD(T)/ac[56]z, all electron	40344(21)
B	CCSDTQP/wc2z, all electron	+8(4)
C	Geometry adjustment	−135(8)
D	Best non-relativistic D_e [=A + B+C]	40218(23)
E	Relativistic correction	−32(3)
F	**Best mass-independent D_e** [=**D** + **E**]	**40188**(**23**)
G	Adiabatic correction (BODC), $^{14}NH_3$	+60(10)
H	**Best mass-dependent D_e** [=**F** + **G**]	**40248**(**25**)
I	Zero point energy NH_3	7433(1)
J	Zero point energy NH_2 [74]	4005(25)
K	Overall zero point energy contribution [=J–I]	−3428(25)
L	**Best theoretical D_0** [=**H** + **K**]	**36820**(**35**)
M	Experimental D_0 [74]	37115(20)
N	Experiment – theory [=M–L]	295(40)

Final values of the dissociation energy D within a certain theoretical model are given in the bold font.

Table 2
Convergence of highly excited levels of NH_3 for different polyad number P_{max} and rectilinear ('rect') or curvilinear ('curv') coordinates. All energies are in cm^{-1}.

P_{max}= Coordinates= Label	28 Rect	28 Curv	32 Curv	36 Curv	40 Curv
A'_1	6798.47	6798.44	6798.33	6798.30	6798.30
A''_2	6796.86	6796.74	6796.68	6796.67	6796.67
E''	6611.54	6610.79	6611.08	6610.67	6610.67
E'	6610.16	6609.85	6609.99	6610.67	6609.73
E'	6666.60	6666.45	6666.44	6666.38	6666.37
E''	6679.58	6679.24	6679.04	6679.16	6679.16
E'	6678.66	6678.55	6678.27	6678.47	6678.47
E''	6852.22	6851.99	6851.97	6851.94	6851.94
E'	6851.69	6851.56	6851.52	6851.51	6851.51
E''	9749.77	9742.15	9744.66	9741.41	9741.40
E' E(s)	9744.54	9740.32	9742.14	9739.86	9739.86
E''	9702.32	9693.64	9697.24	9692.63	9692.62
E' E(s)	9695.72	9692.37	9690.40	9691.72	9691.71
E''	9656.15	9645.99	9649.91	9644.91	9644.90
E' E(a)	9648.85	9642.40	9645.10	9641.72	9641.72
E''	12664.59	12651.93	12652.12	12627.62	12627.56
E' E(av)	12718.80	12683.14	12697.96	12676.55	12676.39
A''_2	15507.56	15527.04	15467.51	15453.04	15446.91
A'_1	15487.20	15497.11	15466.35	15459.60	15458.98
E''	15507.72	15527.15	15467.76	15456.63	15455.64
E'	15487.51	15499.76	15466.82	15458.79	15458.11
A''_2	18292.10	18404.01	18184.72	18127.73	18123.49
A'_1	18262.25	18351.99	18145.72	18115.67	18115.57
E''	18294.78	18410.40	18184.07	18131.45	18122.74
E'	18265.52	18349.18	18145.34	18118.70	18119.42

expect to produce a highly accurate value. We also compare the coupled cluster results with MRCI ones. Because only one NH_3 calculation is required, we could use basis sets which would be too expensive to use for the computation of the full surface. We present in Table 1 a summary of the result and describe the details of the calculation in the following.

Contribution A was computed using both for NH_3 and for NH_2 geometries with r(N–H) = 1.01 Å, ∠HNH = 108°. Calculations of the NH_2 $\tilde{X}\ ^2B_1$ ground state used a restricted open-shell Hartree-Fock reference (RHF) and the UCCSD(T) method [75–77]. The aug-cc-pCV5Z and aug-cc-pCV6Z energies were extrapolated using the formula $E_n = E_\infty + A/(n + 1/2)^4$; the stated uncertainty is one half of the shift of the aug-cc-pCV6Z D_e value to the basis-set extrapolated one.

Contribution B. A high-order coupled cluster correction (up to pentuple excitations [78,79]) was computed using the geometries used for contribution *A* above; the correction is computed as D_e (CCSDTQP) $-D_e$ (CCSD(T)) using the cc-pwCVDZ basis set and correlating all electrons. The reported uncertainty is the absolute value of the difference between the shifts computed in the cc-pwCVDZ and the cc-pVDZ basis sets. Correlation effects beyond CCSDTQP were estimated computing full configuration interaction (FCI) values of D_e in the 6-31G and the cc-pVDZ basis set (frozen core calculations); the CCSDTQP → FCI correction amounts to only +0.1 cm^{-1} using these basis sets and was neglected.

Contribution C. The geometries used in the main calculations (contributions A and B) are not exactly the equilibrium geometries neither for NH_2 nor, to a smaller extent, for NH_3, so we correct for this fact in this step. Using for NH_3 the experimental equilibrium geometry r(N–H) = 1.012 Å, ∠HNH = 106.7° we get using CCSD(T)/aug-cc-pCVQZ-DK (relativistic calculation using the Douglas-Kroll-Hess Hamiltonian to fourth order [80]) a contribution to D_e of +22 cm^{-1}. Using for NH_2 the experimental equilibrium geometry r(N–H) = 1.0254 Å, ∠HNH = 102.85° we get using CCSD(T)/aug-cc-pCV5Z-DK a contribution to D_e of −157 cm^{-1}. The total contribution is therefore +22 − 157 = −135 cm^{-1}. The error bar was established on the basis of comparisons with calculations in smaller basis sets.

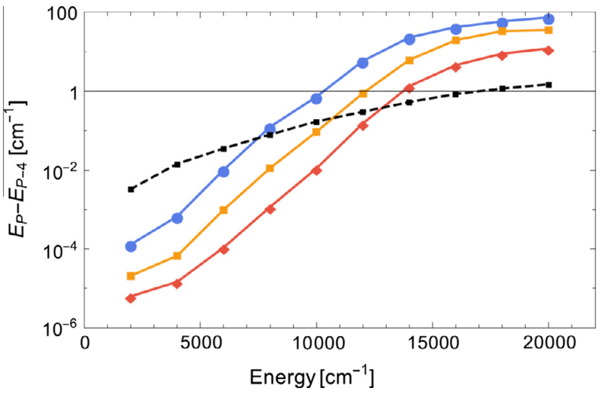

Fig. 1. Basis set convergence of NH_3 vibrational energy levels. The mean absolute energy differences $|E(P_{max}) - E(P_{max} - 4)|$ are drawn in each energy interval (2000 cm^{-1} wide) for three basis sets truncated at polyad numbers $P_{max} = 32, 36$, and 40 in blue circles, orange squares, and red diamonds, respectively. For KEO series truncation errors, the respective differences for $N_{KEO} = 8$ and 6 are drawn as a black dashed line. (For interpretation of the references to colour in this figure legend, the reader is referred to the web version of this article.)

Contribution E. Scalar relativistic corrections were computed by expectation of the mass-velocity one-electron Darwin operator (MVD1) and the MRCI wave function (full valence reference space) in the aug-cc-pCV5Z basis set; the geometries described in contribution *A* above were used. The correction due to quantum electrodynamics was estimated by scaling on the one-electron Darwin term [45], amounts to +2 cm^{-1} and was neglected. The error bar was established on the basis of comparisons with calculations in smaller basis sets and using the Douglas-Kroll-Hess Hamiltonian. The correction due to spin-orbit to D_e is zero to first order of perturbation theory and is therefore negligible ($\ll 1$ cm^{-1}).

Contribution G. The adiabatic correction (also known as the Born-Oppenheimer diagonal correction) was computed using CCSD in the cc-pwCVTZ basis set (all electron calculations) and the program CFOUR [81,82]. The geometries used are the ones described in contribution *A*; the error bar was set on the basis of comparisons with the Hartree-Fock value (which is +52 cm^{-1}) and of the CCSD/cc-pVDZ (frozen core) value (which is +78 cm^{-1}).

Contribution I. The zero point energy of NH_3 was obtained from the new PES produced in this work and was set to 7433(1) cm^{-1};

Table 3
Comparison of calculated ($P_{\max} = 40$) and experimental energy levels of ammonia [10] in cm^{-1}. The column labelled 'obs' are experimental energy levels from Ref. [20], the other columns are differences to calculated values.

v_1	v_2	v_3	v_4	L_3	L_4	L i	Sym.	Obs.	Obs.-calc.[a]	Obs.-calc.[b]	Obs.-calc. [88][c]
0	0	0	0	0	0	0 −	A_2''	0.79	0.03	0.01	0.00
0	1	0	0	0	0	0 −	A_2''	968.12	−3.69	−0.38	−0.01
0	0	0	1	0	1	1 +	E'	1626.27	−1.36	0.09	0.06
0	0	0	1	0	1	1 −	E''	1627.37	−1.31	0.11	0.07
0	2	0	0	0	0	0 −	A_2''	1882.18	−5.67	−0.44	−0.37
0	1	0	1	0	1	1 +	E'	2540.52	−7.14	−1.13	0.22
0	1	0	1	0	1	1 −	E''	2586.13	−5.38	−0.62	0.05
0	3	0	0	0	0	0 −	A_2''	2895.52	−5.64	−0.21	−0.07
0	0	0	2	0	0	0 −	A_2''	3217.59	−2.81	−0.06	−0.69
0	0	0	2	0	2	2 +	E'	3240.16	−3.06	−0.19	−0.45
0	0	0	2	0	2	2 −	E''	3241.60	−3.10	−0.17	−0.43
1	0	0	0	0	0	0 −	A_2''	3337.10	−1.64	−1.50	−1.77
0	0	1	0	1	0	1 +	E'	3443.63	0.03	−0.50	0.27
0	0	1	0	1	0	1 −	E''	3443.99	0.02	−0.50	0.28
1	1	0	0	0	0	0 −	A_2''	4320.03	−5.36	−1.99	−0.19
0	1	1	0	1	0	1 +	E'	4416.92	−4.31	−0.92	−2.27
0	1	1	0	1	0	1 −	E''	4435.45	−3.63	−0.82	−2.36
1	0	0	1	0	1	1 +	E'	4955.76	−3.01	−1.45	−3.79
1	0	0	2	0	2	2 +	E'	6556.42	−4.71	−1.94	−6.52
1	0	0	2	0	2	2 −	E''	6557.93	−4.97	−1.88	−6.75
1	0	1	0	1	0	1 +	E'	6608.82	−2.44	−1.02	−6.05
1	0	1	0	1	0	1 −	E''	6609.75	−2.81	−1.02	−6.18
0	0	1	2	1	2	1 +	E'	6677.43	−1.85	−1.11	
0	0	1	2	1	2	1 −	E''	6678.31	−1.89	−0.92	
0	2	0	3	0	1	1 −	E''	6678.93	−15.53	−2.48	
0	0	2	0	2	0	2	E'	6850.24	−0.45	−1.32	2.52
0	0	2	0	2	0	2	E''	6850.65	−0.47	−1.33	2.53
0	1	0	0	0	0	0 +	A_1'	932.40	−5.01	−0.64	2.52
0	2	0	0	0	0	0 +	A_1'	1597.50	−9.60	−1.12	2.53
0	3	0	0	0	0	0 +	A_1'	2384.20	−6.46	−0.41	
0	0	0	2	0	0	0 +	A_1'	3216.00	−2.69	−0.04	0.17
1	0	0	0	0	0	0 +	A_1'	3336.10	−1.67	−1.52	−0.41
0	4	0	0	0	0	0 +	A_1'	3462.50	−5.54	−0.02	−1.22
0	2	0	1	0	1	1 −	E''	3502.10	−7.93	−1.39	−0.61
0	1	0	2	0	0	0 +	A_1'	4115.60	−10.10	−1.92	−4.00
0	1	0	2	0	2	2 +	E'	4135.90	−9.95	−1.95	1.65
0	1	0	2	0	0	0 −	A_2''	4173.30	−7.33	−0.79	
0	1	0	2	0	2	2 −	E''	4193.10	−7.51	−1.08	−0.39
1	1	0	0	0	0	0 +	A_1'	4294.50	−6.20	−2.16	−0.43
0	2	0	2	0	0	0 +	A_1'	4754.30	−17.61	−5.83	−0.30
0	0	0	3	0	1	1 +	E''	4802.40	−4.14	0.88	−0.44
1	0	0	1	0	1	1 −	E''	4956.90	−3.02	−1.44	3.08
1	2	0	0	0	0	0 +	A_1'	5002.90	−8.52	0.32	
0	0	1	1	1	1	0 +	A_2'	5051.40	−1.57	−0.58	
0	0	1	1	1	1	0 −	A_1''	5052.10	−1.49	−0.48	−4.00
0	2	0	2	0	0	0	A_2''	5092.60	−11.21	−2.61	
0	2	0	2	0	2	2 −	E''	5112.80	−10.87	−2.45	−0.71
0	2	1	0	1	0	1 +	E'	5146.34	−8.38	0.18	−0.57
0	2	1	0	1	0	1 −	E''	5352.80	−6.39	−1.10	
0	2	0	3	0	1	1 +	E'	6310.30	−22.00	−5.43	
2	0	0	0	0	0	0 +	A_1'	6514.10	−9.25	−7.20	
1	0	0	2	0	0	0 +	A_1'	6648.20	−5.86	−3.68	
1	0	0	2	0	0	0 −	A_2''	6649.80	−5.79	−3.21	
0	0	1	2	1	0	0 +	A_2'	6651.40	−2.82	−0.26	
0	0	1	2	1	0	0 −	A_1''	6652.60	−2.92	0.09	
0	0	2	0	0	0	0	A_2''	6792.00	−3.98	−4.73	
0	0	2	0	0	0	0	A_1'	6793.10	−7.71	−5.27	

[a] This work based on the *ab initio* equilibrium geometry.
[b] This work using shifted equilibrium geometry (see Section 4).
[c] Computed by Marquardt et al. [22] using an empirically adjusted potential [89].

this value is in fair agreement with the one computed by Mordaunt et al. of 7415 cm^{-1} from experimental vibrational frequencies and anharmonicity constants.

Contribution J. It is difficult to identify an accurate and reliable value for the zero point energy of the NH_2 radical from the existing literature. Mordaunt et al. [74] use the value 4005 cm^{-1}, which is in fair agreement with the one quoted by Demaison et al. [83] of 48.20 kJ/mol (4029 cm^{-1}). We decided to use the value by Mordaunt et al. and assigned to it an error bar of 25 cm^{-1}. This rather large error bar should also compensate from the fact that the ground state of NH_2 has $J = 1/2$ and not $J = 0$ and because of this computing the zero point energy as 1/2 of the sum of the

Table 4
Comparison of the observed $v_2 = 0$ high energy levels of ammonia (in cm^{-1}) calculated in this work and due to Lehmann and Coy [20]; the second, non-standard symmetry labels are due to Lehmann and Coy.

Sym.	Obs.	Obs.-calc. (this work)	Obs.-calc. [88]
E'	1626.10	−0.08	
A_1'	3336.10	−1.50	
E' E(s)	5052.60	−0.40	
E'' E(a)	5052.97	−0.63	
E' E(s)	6012.90	−1.02	−2.01
E'' E(a)	6037.12	−0.21	−1.53
A_1'	6520	−1.21	−9.40
A_1'	6606.00	−0.14	−11.15
A_1' A(s)	6796.733	−1.57	−15.63
A_2'' A(a)	6795.305	−1.36	−15.36
E'' E(a)	6609.66	−1.01	
E' E(s)	6608.833	−0.90	
E' E	6666	−0.37	
E'' E(a)	6677.95	−1.21	
E' E(s)	6677.229	−1.24	
E'' E(a)	6850.702	−1.24	2.58
E' E(s)	6850.195	−1.32	2.47
E'' E(a)	9738.839	−2.56	
E' E(s)	9738.15	−1.70	
E'' E(a)	9689.722	−2.89	
E' E(s)	9689.84	−1.87	
E'' E(a)	9642.323	−2.58	−6.96
E' E(a)	9639.652	−2.06	−7.49
E'' E(av)	12628.20	0.64	
E' E(av)	12675.50	−0.89	
A_2'' A(a)	15447.38	0.47	
A_1' A(s)	15450.82	−8.16	
E'' E(a)	15448.70	−6.94	
E' E(s)	15451.19	−6.92	
A_2'' A(a)	18109.18	−14.31	
A_1' A(s)	18109.47	−6.10	
E'' E(a)	18107.56	−15.18	
E' E(s)	18109.47	−9.95	

Table 5
Vibrational term values of $H_2{}^{16}O$ computed *ab initio* using the same model employed for NH_3. Observed from the IUPAC [90].

v_1	v_2	v_3	Obs.	Calc. 1	Obs.-calc.	Calc. 2	Obs.-calc.
0	1	0	1594.75	1595.56	−0.81	1595.18	−0.44
0	2	0	3151.63	3152.98	−1.35	3152.19	−0.56
1	0	0	3657.05	3658.65	−1.59	3658.60	−1.54
0	0	1	3755.93	3757.54	−1.61	3756.60	−0.67
1	1	0	5234.98	5237.36	−2.38	5236.93	−1.96
0	1	1	5331.27	5333.59	−2.32	5332.30	−1.03
1	2	0	6775.09	6777.95	−2.85	6777.11	−2.02
0	2	1	6871.52	6874.30	−2.78	6872.62	−1.10
2	0	0	7201.54	7204.30	−2.76	7204.23	−2.69
1	0	1	7249.82	7252.57	−2.76	7251.59	−1.77
0	0	2	7445.06	7448.13	−3.08	7448.24	−3.18
2	1	0	8761.58	8765.12	−3.54	8764.68	−3.10
1	1	1	8807.00	8810.50	−3.50	8809.17	−2.17
0	1	2	9000.14	9003.91	−3.77	9003.67	−3.53
2	2	0	10284.36	110288.40	−4.03	10287.56	−3.20
1	2	1	10328.73	110332.71	−3.98	10330.99	−2.26
0	2	2	10521.76	110525.97	−4.21	10525.36	−3.60
3	0	0	10599.69	110603.54	−3.85	10603.49	−3.80
2	0	1	10613.36	110617.07	−3.72	10616.07	−2.71
1	0	2	10868.87	110873.12	−4.24	10873.10	−4.23
0	0	3	11032.40	111036.44	−4.03	11035.59	−3.19
3	1	0	12139.32	112144.21	−4.89	12143.80	−4.48
2	1	1	12151.25	112156.03	−4.78	12154.67	−3.42
1	1	2	12407.66	112412.62	−4.96	12412.23	−4.57
0	1	3	12565.01	112569.73	−4.73	12568.57	−3.56
3	2	0	13640.72	113646.23	−5.51	13645.21	−4.50
2	2	1	13652.65	113658.18	−5.53	13656.47	−3.81
4	0	0	13828.27	113834.32	−6.04	13834.28	−6.01
3	0	1	13830.94	113836.85	−5.92	13833.95	−3.01
1	2	2	13910.89	113916.41	−5.52	13915.66	−4.76
0	2	3	14066.19	114071.42	−5.23	14069.92	−3.73
2	0	2	14221.16	114226.98	−5.82	14226.89	−5.73
1	0	3	14318.81	114323.88	−5.07	14322.95	−4.14
0	0	4	14537.50	114542.12	−4.61	14542.31	−4.81
4	1	0	15344.50	115352.35	−7.85	15351.93	−7.42

harmonic frequencies plus anharmonicity corrections (formula 4 of Ref. [74]) is not a fully correct procedure.

As one can see from the values in Table 1 there is a strong discrepancy (by more than 7σ) between our calculated value for D_0 and the experimentally-derived value from Ref. [74]. The reason for this disagreement is at the moment unknown.

We also computed values of D_e using MRCI. For this method we can compute D_e either by performing separate equilibrium calculations for NH_3 and for NH_2 and H as in the coupled cluster case or, alternatively, by performing a two-point calculation for NH_3, one at equilibrium and one where one of the N–H bonds is highly stretched. As MRCI is not a size consistent method we expect in principle different results for the two strategies; however, tests in the cc-pVDZ basis set and the full valence reference space showed that the size consistency error (i.e., the difference in D_e between the two way of computing it) is only about 0.01 cm^{-1} both for MRCI and MRCI+Q energies and therefore completely negligible. We also tested the difference between energies computed using the Werner-Knowles internal contraction scheme [56] or the newer and faster Celani-Werner one [57,62]; once again tests in the cc-pVDZ and the full valence reference space showed that the two schemes produce energy curves differing by less than 0.01 cm^{-1} along the whole stretching curve, so both contraction scheme are equivalent in practice. With respect to the best non-relativistic coupled-cluster value (quantity D in Table 1) the MRCI value in the full valence reference space is 314 cm^{-1} lower while the Davidson-corrected MRCI+Q (fixed reference) is 23 cm^{-1} lower. Using a larger reference space with two extra orbitals the MRCI value is 295 cm^{-1} lower than the best coupled cluster based one and MRCI+Q is 53 cm^{-1} lower. Overall we consider the agreement of the MRCI+Q energies very good, especially in the full valence reference space. This observation implies than MRCI+Q is capable of providing very high accuracy all the way up to dissociation.

4. Nuclear motion calculations

Rotation-vibrational energy levels were calculated using the general, variational program TROVE [23,24]. In TROVE the ro-vibrational Hamiltonian is expressed in terms of internal valence coordinates as a Taylor series expansion around a non-rigid reference configuration and is represented explicitly on a grid. The expansion coefficients for the kinetic energy operator (KEO) and the PES are obtained in a numerically exact fashion using automatic differentiation techniques. [24] In the present work, the kinetic and potential energy operators were expanded up to 8-th order in terms of the N–H$_i$ ($i = 1, 2, 3$) stretching coordinates and of the symmetry-adapted bending coordinates

$$s_4 = \frac{1}{\sqrt{6}}(2\beta_{23} - \beta_{13} - \beta_{12}),$$

$$s_5 = \frac{1}{\sqrt{2}}(\beta_{13} - \beta_{12}),$$

where β_{ij} is the $\angle(H_i\text{–}N\text{–}H_j)$ bending angle projected on the plane perpendicular to the trisector vector. We choose to work with s_4 and s_5 given in terms of β_{ij} rather than $\angle(H_i\text{–}N\text{–}H_j)$ considering their relatively simple relations to the Cartesian coordinates of the atoms, which is highly desirable for the automatic procedure of constructing the KEO in TROVE. For the expansion of the potential energy we

Table 6
Calculated vibrational transition moments of ammonia molecule. All the transitions are from ground state, so freq. = E_{up}; $v_{\mathrm{str}} = v_1 + v_3$ is the total stretching excitation; Sym. is the irreducible representation in the $D_{3h}(M)$ group; int. is the vibrational band intensity in cm/molecule.

Freq.	Int.	v_{str}	v_2	v_4	Sym.
12619.65	1.47E−28	3	1	1	E'
12627.15	1.31E−28	3	3	0	A_2''
12628.69	1.71E−28	4	0	0	A_2''
12628.85	1.98E−38	3	0	1	A_1''
12629.26	8.29E−28	4	0	0	E'
12633.02	1.50E−29	1	6	2	E'
12642.14	8.34E−29	3	1	1	A_2''
12651.06	6.26E−29	3	3	0	E'
12661.57	1.02E−28	1	3	4	A_2''
12655.96	1.83E−28	0	0	8	E'
12677.15	7.12E−28	4	0	0	E'
12678.37	2.04E−28	2	6	0	E'
12679.10	2.74E−28	4	0	0	A_2''
12698.93	3.45E−28	1	2	5	E'
15400.22	7.64E−30	0	0	3	A_2''
15402.91	2.61E−31	0	0	1	E'
15407.52	4.27E−32	0	0	0	A_2''
15412.47	2.52E−30	0	2	2	A_2''
15417.96	5.99E−30	0	0	2	A_2''
15422.55	1.25E−29	0	0	2	E'
15431.20	7.54E−32	0	0	2	E'
15440.54	4.92E−30	1	1	0	A_2''
15443.00	1.03E−29	0	0	2	E'
15446.12	1.31E−29	0	0	1	E'
15448.62	7.52E−29	0	0	0	A_2''
15452.93	3.69E−29	1	1	0	E'
15457.13	1.86E−29	0	0	1	A_2''
15458.46	2.62E−29	0	0	2	E'
15460.30	2.01E−28	0	5	0	E'
15461.13	2.06E−28	5	0	0	A_2''
15462.61	5.03E−28	0	5	0	E'
15464.40	1.64E−28	0	0	2	E'
15465.75	7.62E−29	0	0	2	E'
15471.34	2.08E−30	0	0	3	A_2''
15472.54	8.27E−29	2	1	1	E'
15479.57	6.59E−30	0	0	2	E'
15483.25	2.16E−29	0	0	1	E'
15484.95	1.57E−29	0	0	1	E'
18100.82	3.74E−29	3	1	0	E'
18102.36	2.77E−32	1	1	0	A_2''
18104.85	4.05E−29	3	0	1	E'
18105.09	9.47E−31	1	1	0	A_2''
18107.96	7.94E−31	1	0	2	A_2''
18112.67	2.16E−30	2	0	2	E'
18118.74	3.20E−30	1	0	2	E'
18121.44	1.08E−29	1	1	0	E'
18124.62	1.17E−28	6	0	0	E'
18126.44	9.96E−29	6	0	0	E'
18128.48	6.89E−30	0	0	3	A_2''
18130.57	1.05E−28	6	0	0	E'
18131.58	1.06E−28	6	0	0	A_2''
18132.40	1.00E−28	6	0	0	E'
18133.07	1.36E−30	0	2	2	A_2''
18136.10	4.82E−29	3	1	1	E'
18137.51	3.37E−31	0	0	3	A_2''
18137.77	3.57E−29	3	1	1	E'
18141.69	7.32E−30	0	0	1	A_2''
18147.69	3.77E−30	1	0	2	E'
18150.55	7.69E−30	1	0	2	E'

employed Morse-type variables for the three stretching coordinates. The non-rigid reference configuration was defined by the umbrella-motion vibrational coordinate τ on a grid of 1000 points with displacements covering potential energies up to 40 000 cm^{-1} above the minimum.

Table 7
Vibrational energy levels of the NH_2D molecule.

Sym.	Obs.	Obs.-calc. (this work)	Obs.-calc. [88]
A−	0.41	0.00	0.01
A+	876.37	−0.52	0.00
A−	896.56	−0.38	0.00
B+	1389.91	0.05	0.13
B−	1390.50	0.05	0.14
A−	1591	0.02	0.28
A+	1605.64	−0.06	0.02
A−	2505.9	−1.24	1.26
A+	2506.51	−1.23	1.01
A+	3365.24	−1.32	5.56
A−	3367.59	−1.27	4.29
B+	3438.86	−0.90	−0.27
B−	3439.03	−0.94	−0.27

Table 8
Vibrational energy levels of the NHD_2 molecule.

Sym.	Obs.	Obs.-calc. (this work)	Obs.-calc. [88]
A−	0.171	0.00	0.00
A+	810.23	−0.39	0.01
A−	819.56	−0.34	−0.02
A+	1233.37	−0.02	0.26
A−	1235.89	0.01	0.24
B+	1461.79	0.06	0.22
B−	1461.99	0.03	0.21
A+	2430.80	−0.94	0.69
A−	2434.62	−1.00	0.55
B+	2559.81	−1.52	1.82
B−	2559.96	−1.54	1.82
A−	3404.24	−1.68	−2.86
A+	3404.32	−1.45	−3.03

The general variational solution in TROVE involves several steps (basis set optimization, contraction, symmetrization) described in general elsewhere [23,24] and in Ref. [16] for NH_3 in particular. The size of the total vibrational basis set is controlled by the polyad number P

$$P = 2(n_{\mathrm{NH}_1} + n_{\mathrm{NH}_2} + n_{\mathrm{NH}_3}) + n_{s_4} + n_{s_5} + \frac{n_\tau}{2},$$

with n_i denoting the quantum numbers of the corresponding primitive basis functions, which restricts the products of the primitive functions to those for which $P \leqslant P_{\max}$. In the present calculation we employed $P_{\max} = 40$.

The original implementation of TROVE performed calculations using rectilinear coordinates. However, during the course of this work a new version based on the use of curvilinear coordinates became available [84]. In particular, rectilinear coordinates, as illustrated by the first column of Table 2, when used with $P_{\max} = 28$ resulted in a large discrepancy with the highest experimentally known energy levels at about 18 000 cm^{-1} of about 100 cm^{-1}. The use of curvilinear coordinates permitted the use of polyad numbers up to 40 and therefore allowed for much better convergence. The values of the parameters r_{eq} and α_{eq} were determined during the fitting of *ab initio* points as 1.0106 Å and 106.696°. However, we find better agreement with experiment if we shift these values slightly to 1.0116 Å and 106.719°. The calculated energy levels in Table 2 were obtained with these shifted values.

To assess the accuracy of the variational setup employed in this study we performed calculations with basis sets of different sizes. We report in Table 2 energy levels calculated with different values of the truncation parameter $P_{\max}$. Calculations $P_{\max} = 28$ were carried out with the linearised coordinates, while calculations with $P_{\max} > 28$ used curvilinear ones.

Fig. 1 plots the mean absolute differences between energies calculated with polyad number $P_{\max}$ and $(P_{\max} - 4)$ in energy intervals of 2000 cm^{-1}. All states with energies below 20000 cm^{-1} and an absolute value of the leading coefficient in the wave function larger than 0.5 were selected for the plot, resulting in about 1200 in number. Gradual increase of the basis set improves the accuracy by about one order of magnitude for energies below 14000 cm^{-1}, while for higher energies the curves on Fig. 1 show almost the same convergence rates for all states up to 20000 cm^{-1}. This is due to the heavy mixing of states at higher energies, so that only few of them passed the threshold for the leading coefficient and were considered in the plot, fictitiously lowering the average errors. By extrapolating the convergence pattern between 6000 and 14000 cm^{-1} to higher energies it can be seen that to obtain an accuracy of 1 cm^{-1} for all energy levels below 20000 cm^{-1} the basis set should be extended to at least $P_{\max} = 48$.

5. Rovibrational energy levels of NH_3 and isotopologues

Table 3 compares the results of $J = 0$ calculations on $^{14}NH_3$ with the $J = 0$ energy levels, obtained in Ref. [10] using the MARVEL procedure [85,86]. The table substantiates our claim that we can reproduce the energy levels of NH_3 to within 1 cm^{-1}.

Table 4 presents a comparison of our calculations with the measured energy levels of highly-excited stretching ($v_2 = 0$) levels up to 18000 cm^{-1}. These energies were obtained by Coy and Lehmann quite some time ago [19,20], but there are no previous attempts to reproduce these levels from first principles. Comparing these results with the ones for water computed at the same level of theory, see Table 5, one finds that the results are very similar. Note that the calculated water levels used slightly shifted equilibrium parameters, just like the ammonia ones (see Section 4).

The correctness of the calculated levels of Table 4 (and of the labelling of the experimental energy levels in Table 2) was also confirmed by calculations of vibrational band intensities, shown in Table 6. In experiment usually the strongest bands are visible. Therefore, quantum numbers of the strongest lines from Table 6 were taken, corresponding to transitions from the ground vibrational state to the energy levels with strong stretch excitation. These calculated levels (and quantum number) were substituted into Tables 2 and 4.

Table 9
Vibrational energy levels of the ND_3 molecule.

Sym.	Obs.	Obs.-calc. (this work)	Obs.-calc. [88]
A2−	0.053	0.00	0.00
A1+	745.6	−0.34	−0.12
A2−	749.14	−0.33	−0.13
E+	1191.49	1.00	1.23
E−	1191.56	1.00	1.23
A1+	1359	−0.96	0.38
A2−	1429	−1.63	−0.60
A1+	1830	2.56	3.22
A2−	2106.6	−0.89	0.04
A1+	2359	4.01	
A2−	2359	3.63	
A1+	2420.11	−1.21	1.53
A2−	2420.65	−1.21	1.53
A1+	2482	0.54	1.42
E−	2563.91	−1.79	1.95
E+	2563.93	−1.74	1.95
A2−	2876	4.08	6.04
A1+	3093.01	−1.23	0.97
A2−	3099.46	−0.50	1.62
A1+	3171.89	−1.80	4.28
A2−	3175.87	−1.73	3.91
E+	3327.94	−2.07	0.14
E−	3329.56	−2.10	0.12
E+	4887.29	−2.64	−0.28
E−	4887.67	−2.83	−0.34
E-	4938.44	−2.88	−0.77
E+	4938.44	−2.62	−0.95
E+	5100.66	−3.39	4.42
E−	5100.66	−3.40	4.40

Table 10
Vibrational energy levels of the $^{15}NH_3$ molecule.

Sym.	Obs. [91]	Calc.	Obs.-calc.
A_2''	0.761	0.76	0.01
A_1'	928.509	929.05	−0.54
A_2''	962.912	963.27	−0.36
A_1'	1591.236	1592.34	−1.10
E'	1623.13	1623.07	0.06
E''	1624.19	1624.12	0.07
A_2''	1870.823	1871.30	−0.47
A_1'	2369.274	2369.77	−0.49
E'	2533.382	2534.58	−1.19
E''	2577.571	2578.32	−0.75
A_2''	2876.144	2876.32	−0.18
A_1'	3210.614	3210.79	−0.18
A_2''	3212.335	3212.49	−0.15
E'	3234.107	3234.23	−0.12
E''	3235.504	3235.71	−0.21
A_1'	3333.306	3334.75	−1.44
A_2''	3334.252	3335.74	−1.49
E'	3435.167	3435.62	−0.45
E''	3435.54	3435.98	−0.44
A_1'	4288.186	4290.16	−1.98
A_2''	4312.345	4314.30	−1.95
E'	6546.951	6548.99	−2.03
E''	6548.56	6550.75	−2.19
E'	6596.569	6597.99	−1.42
E''	6597.607	6599.33	−1.72
E'	6664.486	6665.52	−1.03
E''	6665.48	6666.01	−0.53

Table 11
Comparison of the newly analysed band origins around 8000 cm^{-1} taken from [87] with our calculations.

Sym. exp	Observed [87]	Obs.-calc.	Obs.-calc. (our)
$v_1 + v_2 + 2v_4^2$ s	7573.282	2.6	3.88
$v_1 + v_2 + 2v_3^3$ s	7658.485	2.2	−0.47
$v_1 + v_2 + 2v_3^3$ a	7675.113	2.3	−0.37
$v_2 + 2v_3^2$ s	7854.539	3.0	−1.58
$v_2 + 2v_3^2$ a	7864.078	2.4	−1.69

Further comparison of the accuracy of the present calculations with the highly excited energy levels of NH_3 became possible during the course of this work thanks to new assignments of highly excited ammonia states close to 8000 cm^{-1} [87]. In particular, the band origins of 5 highly excited vibrational states of ammonia have been determined from the new analysis of experimental data [87], see Table 11. As it can be seen from the table, four out of the five presented highly excited band origins are reproduced by our *ab initio* calculations within 2 cm^{-1}, which is even more accurate than the semiempirical predictions of the BYTe linelist [17]. This confirms once more the accuracy of our PES and its ability to calculate highly excited vibrational states of ammonia.

Predicted energy levels for isotopically substituted NH_3 were also computed. Results for NH_2D, NHD_2, ND_3 and $^{15}NH_3$ are presented in Tables 7–10 respectively. All isotopologues calculations were made with $P_{\max} = 28$ and linearised TROVE coordinates.

6. Conclusion

In this paper we have achieved an accuracy of about 1 cm^{-1} for all levels up to 7000 cm^{-1} given in the comprehensive compilation of experimental levels [10] and an accuracy between 2 and 10 cm^{-1} for levels up to 18000 cm^{-1} measured by Lehmann and Coy [20]. This *ab initio* PES should therefore serve as an excellent starting point for semi-empirical fits which may provide even more accurate line positions in both infrared and visible regions.

We also estimate the dissociation energy of NH_3 by two independent theoretical procedures and with significantly improved accuracy compared to previous theoretical determinations; however, there is a discrepancy with experiment which requires further investigation. The paper constitutes a first step towards a global, high-accuracy *ab initio* PES of ammonia. Our work should also pave the way towards the to observation and analysis of the predissociation spectra of NH_3 analogous to what could have been achieved for water, only, up until now [92–95].

For the present study the availability of *ab initio* results for water at various level of theory (i.e., including only some of the components discussed in Section 2.1 or using smaller basis sets) including the very accurate one from Refs. [25,92,96] proved very useful; in particular, we confirmed that use of analogous levels of theory for water and ammonia leads to similar errors in rovibrational energy levels; we are therefore confident that very accurate results – similar in quality to the ones for water of Ref. [25] – can be obtained for ammonia as well as for other 10 electron molecules, such as methane. The computationally more onerous step for future calculations is the extension to the larger aug-cc-pCV6Z basis set, although the use of explicitly-correlated methods and the cc-pV5Z-F12 basis set may provide a valid, cheaper alternative. It will also be necessary to consider relativistic corrections based on the Breit-Coulomb Hamiltonian, quantum electrodynamics corrections as well as a more extensive treatment of nonadiabatic correction such as the one used by Huang et al. [14]. It is expected that once these corrections are implemented accuracies of the order of 0.1 cm^{-1} should be achievable *ab initio* for excited rotation-vibration levels.

Acknowledgement

This work was supported by the ERC Advanced Investigator Project 267219, the UK Natural Environment Research Council and the Russian Fund for Fundamental Studies. The State Project IAP RAS No. 0035-2014-009 is acknowledged by RIO, AAK, and NFZ.

Appendix A. Supplementary material

Supplementary data associated with this article can be found, in the online version, at http://dx.doi.org/10.1016/j.jms.2016.08.003.

References

[1] J.W. Erisman, J.N. Galloway, S. Seitzinger, A. Bleeker, N.B. Dise, A.M.R. Petrescu, A.M. Leach, W. de Vries, Phil. Trans. Roy. Soc. London B 368 (2013).
[2] K. von Bobrutzki, C.F. Braban, D. Famulari, S.K. Jones, T. Blackall, T.E.L. Smith, M. Blom, H. Coe, M. Gallagher, M. Ghalaieny, et al., Atmos. Meas. Tech. 3 (2010) 91.
[3] P.W. Lucas, C.G. Tinney, B. Burningham, S.K. Leggett, D.J. Pinfield, R. Smart, H.R. A. Jones, F. Marocco, R.J. Barber, S.N. Yurchenko, et al., Mon. Not. R. Astron. Soc. 408 (2010) L56.
[4] S.K. Leggett, C.V. Morley, M.S. Marley, D. Saumon, Astrophys. J. 799 (2015) 37.
[5] J.P. Beaulieu, G. Tinetti, D. Kipping, I. Ribas, R.J. Barber, J.Y.-K. Cho, I. Polichtchouk, J. Tennysson, S.N. Yurchenko, C.A. Griffith, et al., Astrophys. J. 731 (2011) 16.
[6] N.F. Zobov, S.V. Shirin, R.I. Ovsyannikov, O.L. Polyansky, S.N. Yurchenko, R.J. Barber, J. Tennyson, R. Hargreaves, P. Bernath, J. Mol. Spectrosc. 269 (2011) 104.
[7] R.J. Hargreaves, G. Li, P.F. Bernath, J. Quant. Spectrosc. Radiat. Transf. 113 (2012) 670.
[8] R.J. Hargreaves, G. Li, P.F. Bernath, Astrophys. J. 735 (2012) 111.
[9] E.J. Barton, S.N. Yurchenko, J. Tennyson, S. Clausen, A. Fateev, J. Quant. Spectrosc. Radiat. Transf. 167 (2015) 126.
[10] A.R. Al Derzi, T. Furtenbacher, S.N. Yurchenko, J. Tennyson, A.G. Császár, J. Quant. Spectrosc. Radiat. Transf. 161 (2015) 117.
[11] T. Rajamäki, A. Miani, L. Halonen, J. Chem. Phys. 118 (2003) 10929.
[12] T. Rajamäki, M. Kállay, T. Noga, P. Valiron, L. Halonen, Mol. Phys. 102 (2004) 2297.
[13] X. Huang, D.W. Schwenke, T.J. Lee, J. Chem. Phys. 129 (2008) 214304.
[14] X. Huang, D.W. Schwenke, T.J. Lee, J. Chem. Phys. 134 (2011) 044320.
[15] X. Huang, D.W. Schwenke, T.J. Lee, J. Chem. Phys. 134 (2011) 044321.
[16] S.N. Yurchenko, R.J. Barber, A. Yachmenev, W. Thiel, P. Jensen, J. Tennyson, J. Phys. Chem. A 113 (2009) 11845.
[17] S.N. Yurchenko, R.J. Barber, J. Tennyson, Mon. Not. R. Astron. Soc. 413 (2011) 1828.
[18] S.N. Yurchenko, R.J. Barber, J. Tennyson, W. Thiel, P. Jensen, J. Mol. Spectrosc. 268 (2011) 123.
[19] S.L. Coy, K.K. Lehmann, J. Chem. Phys. 84 (1986) 5239.
[20] K.K. Lehmann, S.L. Coy, J. Chem. Soc. Faraday Trans. II 84 (1988) 1389.
[21] C. Sousa-Silva, N. Hesketh, S.N. Yurchenko, C. Hill, J. Tennyson, J. Quant. Spectrosc. Radiat. Transf. 142 (2014) 66.
[22] R. Marquardt, K. Sagui, J. Zheng, W. Thiel, D. Luckhaus, S. Yurchenko, F. Mariotti, M. Quack, J. Phys. Chem. A 117 (2013) 7502.
[23] S. Yurchenko, P. Jensen, W. Thiel, J. Chem. Phys. 71 (2004) 281.
[24] S. Yurchenko, P. Jensen, W. Thiel, J. Chem. Phys. 90 (2010) 333.
[25] O.L. Polyansky, R.I. Ovsyannikov, A.A. Kyuberis, L. Lodi, J. Tennyson, N.F. Zobov, J. Phys. Chem. A 117 (2013) 96339643.
[26] A. Kyuberis, L. Lodi, N. Zobov, O. Polyansky, J. Mol. Spectrosc. 316 (2015) 38.
[27] P. Szalay, T. Müller, G. Gidofalvi, H. Lischka, R. Shepard, Chem. Rev. 112 (2012) 108.
[28] T.H. Dunning Jr., J. Chem. Phys. 90 (1989) 1007.
[29] D.E. Woon, T.H. Dunning Jr., J. Chem. Phys. 103 (1995) 4572.
[30] K.A. Peterson, T.H. Dunning Jr., J. Chem. Phys. 117 (2002) 10548 (13 pages).
[31] D. Feller, J. Chem. Phys. 138 (2013) 074103.
[32] D. Feller, K.A. Peterson, J.G. Hill, J. Chem. Phys. 135 (2011) 044102.
[33] K.A. Peterson, D. Feller, D.A. Dixon, Theor. Chem. Acc. 131 (2012) 1079.
[34] M. Pavanello, L. Adamowicz, A. Alijah, N.F. Zobov, I.I. Mizus, O.L. Polyansky, J. Tennyson, T. Szidarovszky, A.G. Császár, M. Berg, et al., Phys. Rev. Lett. 108 (2012) 023002.
[35] M. Pavanello, L. Adamowicz, A. Alijah, N.F. Zobov, I.I. Mizus, O.L. Polyansky, J. Tennyson, T. Szidarovszky, A.G. Császár, J. Chem. Phys. 136 (2012) 184303.
[36] X. Huang, R.S. Freedman, S.A. Tashkun, D.W. Schwenke, T.J. Lee, J. Quant. Spectrosc. Radiat. Transf. 130 (2013) 134.
[37] L. Lodi, J. Tennyson, O.L. Polyansky, J. Chem. Phys. 135 (2011) 034113.
[38] G. Tarczay, A.G. Császár, W. Klopper, H.M. Quiney, Mol. Phys. 99 (2001) 1769.
[39] A.G. Császár, J.S. Kain, O.L. Polyansky, N.F. Zobov, J. Tennyson, Chem. Phys. Lett. 293 (1998) 317. erratum 312 (1999) 613–616.
[40] P. Pyykkö, Chem. Rev. 112 (2012) 371.
[41] J. Autschbach, J. Chem. Phys. 136 (2012) 150902.
[42] H.M. Quiney, P. Barletta, G. Tarczay, A.G. Császár, O.L. Polyansky, J. Tennyson, Chem. Phys. Lett. 344 (2001) 413.
[43] P. Pyykkö, Adv. Quantum Chem. 11 (1978) 353.
[44] L. Lodi, O.L. Polyansky, A.A.J. Tennyson, N.F. Zobov, Phys. Rev. A 89 (2014) 032505.
[45] P. Pyykkö, K.G. Dyall, A.G. Császár, G. Tarczay, O.L. Polyansky, J. Tennyson, Phys. Rev. A 63 (2001) 024502.
[46] O.L. Polyansky, J. Tennyson, J. Chem. Phys. 110 (1999) 5056.
[47] P.R. Bunker, R.E. Moss, J. Mol. Spectrosc. 80 (1980) 217.
[48] D.W. Schwenke, J. Phys. Chem. A 105 (2001) 2352.
[49] S.P.A. Sauer, J.F. Ogilvie, J. Phys. Chem. 98 (1994) 8617.
[50] J.F. Ogilvie, J. Oddershede, S.P.A. Sauer, Adv. Chem. Phys. 111 (2000) 475.
[51] N.F. Zobov, S.V. Shirin, L. Lodi, B.C. Silva, J. Tennyson, A.G. Császár, O.L. Polyansky, Chem. Phys. Lett. 507 (2011) 48.
[52] C.M. Marian, Rev. Comp. Chem. 17 (2001) 99.
[53] C.M. Marian, WIREs Comput. Mol. Sci. 2 (2012) 187.
[54] R.J. Gdanitz, R. Ahlrichs, Chem. Phys. Lett. 143 (1988) 413.
[55] P.G. Szalay, R.J. Bartlett, J. Chem. Phys. 103 (1995) 3600.
[56] H.-J. Werner, P.J. Knowles, J. Chem. Phys. 89 (1988) 5803.
[57] G.K.K.R. Shamasundar, H.-J. Werner, J. Chem. Phys. 135 (2011) 054101.
[58] D.I. Lyakh, V.F.L.M. Musiał, R.J. Bartlett, Chem. Rev. 112 (2012) 182.
[59] Z. Rolik, M. Kállay, J. Chem. Phys. 141 (2014) 134112.
[60] P. Barker, S.M. Purcell, P. Douglas, P. Barletta, N. Coppendale, C. Maher-McWilliams, J. Tennyson, Faraday Discuss. 142 (2009) 175.
[61] K. Sung, L.R. Brown, X. Huang, D.W. Schwenke, T.J. Lee, S.L. Coy, K.K. Lehmann, J. Quant. Spectrosc. Radiat. Transfer 113 (2012) 1066.
[62] P. Celani, H.-J. Werner, J. Chem. Phys. 112 (2000) 5546.
[63] S. Yurchenko, J. Zheng, H. Lin, P. Jensen, W. Thiel, J. Chem. Phys. 123 (2005) 134308.
[64] H. Lin, W. Thiel, S. Yurchenko, M. Carvajal, P. Jensen, J. Chem. Phys. 117 (2002) 11265.
[65] S.N. Yurchenko, W. Thiel, P. Jensen, J. Mol. Spectrosc. 240 (2006) 174.
[66] S.N. Yurchenko, P.R. Bunker, P. Jensen, J. Molec. Struct. (THEOCHEM) 742 (2005) 43.
[67] R.I. Ovsyannikov, W. Thiel, S.N. Yurchenko, M. Carvajal, P. Jensen, J. Mol. Spectrosc. 252 (2008) 121.
[68] S.N. Yurchenko, W. Thiel, M. Carvajal, P. Jensen, Contemp. Phys. 346 (2008) 146.
[69] D.S. Underwood, J. Tennyson, S.N. Yurchenko, Phys. Chem. Chem. Phys. 15 (2013) 10118.

[70] O.V. Boyarkin, M.A. Koshelev, O. Aseev, P. Maksyutenko, T.R. Rizzo, N.F. Zobov, L. Lodi, J. Tennyson, O.L. Polyansky, Chem. Phys. Lett. 568–569 (2013) 14.

[71] D.K. Bohme, R.S. Hemsworth, H.W. Rundle, J. Chem. Phys. 59 (1973) 77.

[72] S.T. Gibson, J.P. Greene, J. Berkowitz, J. Chem. Phys. 83 (1985) 4319.

[73] F. Qi, L. Sheng, Y. Zhang, S. Yu, W.-K. Li, Chem. Phys. Lett. 234 (1995) 450.

[74] D.H. Mordaunt, R.N. Dixon, M.N.R. Ashfold, J. Chem. Phys. 104 (1996) 6472.

[75] P.J. Knowles, C. Hampel, H.-J. Werner, J. Chem. Phys. 99 (1993) 5219.

[76] P.J. Knowles, C. Hampel, H.-J. Werner, J. Chem. Phys. 112 (2000) 3106.

[77] H.-J. Werner, P.J. Knowles, G. Knizia, F.R. Manby, M. Schütz, P. Celani, T. Korona, R. Lindh, A. Mitrushenkov, G. Rauhut, et al., Molpro, version 2012.1, a package of ab initio programs, 2012, see <http://www.molpro.net>.

[78] MRCC, MRCC, a string-based quantum chemical program suite written by M. Kállay, see <http://www.mrcc.hu>.

[79] M. Kállay, P.R. Surján, J. Chem. Phys. 115 (2001) 2945.

[80] M. Reiher, Theor. Chem. Acc. 116 (2006) 241.

[81] J. Stanton, J. Gauss, M. Harding, P. Szalay, A. Auer, R. Bartlett, U. Benedikt, C. Berger, D. Bernholdt, Y. Bomble, et al., Cfour, a quantum chemical program package, For the current version, 2009, see <http://www.cfour.de>.

[82] J. Gauss, A. Tajti, M. Kállay, J.F. Stanton, P.G. Szalay, J. Chem. Phys. 125 (2006) 144111.

[83] J. Demaison, L. Margulès, J.E. Boggs, Phys. Chem. Chem. Phys. 5 (2003) 3359.

[84] A. Yachmenev, S.N. Yurchenko, J. Chem. Phys. 143 (2015) 014105.

[85] T. Furtenbacher, A.G. Császár, J. Tennyson, J. Mol. Spectrosc. 245 (2007) 115.

[86] T. Furtenbacher, A.G. Császár, J. Quant. Spectrosc. Radiat. Transf. 113 (2012) 929.

[87] E.J. Barton, S.N. Yurchenko, J. Tennyson, S. Béguier, Alain Campargue, J. Mol. Spectrosc. 325 (2016) 7.

[88] R. Marquardt, K. Sagui, J. Zheng, W. Thiel, D. Luckhaus, S. Yurchenko, F. Mariotti, M. Quack, J. Phys. Chem. A 117 (2013) 7502.

[89] S.N. Yurchenko, J. Zheng, H. Lin, P. Jensen, W. Thiel, J. Chem. Phys. 123 (2005) 134308.

[90] J. Tennyson, P.F. Bernath, L.R. Brown, A. Campargue, M.R. Carleer, A.G. Császár, L. Daumont, R.R. Gamache, J.T. Hodges, O.V. Naumenko, et al., J. Quant. Spectrosc. Radiat. Transf. 117 (2013) 29.

[91] S.N. Yurchenko, J. Quant. Spectrosc. Radiat. Transf. 152 (2015) 28.

[92] M. Grechko, O.V. Boyarkin, T.R. Rizzo, P. Maksyutenko, N.F. Zobov, S. Shirin, L. Lodi, J. Tennyson, A.G. Császár, O.L. Polyansky, J. Chem. Phys. 131 (2009) 221105.

[93] A.G. Császár, E. Mátyus, L. Lodi, N.F. Zobov, S.V. Shirin, O.L. Polyansky, J. Tennyson, J. Quant. Spectrosc. Radiat. Transf. 111 (2010) 1043.

[94] P. Maksyutenko, N.F. Zobov, S.V. Shirin, O.L. Polyansky, J.S. Muenter, T.R. Rizzo, O.V. Boyarkin, J. Chem. Phys. 126 (2007) 241101.

[95] M. Grechko, P. Maksyutenko, N.F. Zobov, S.V. Shirin, O.L. Polyansky, T.R. Rizzo, O.V. Boyarkin, J. Phys. Chem. A 112 (2008) 10539.

[96] D.S. Makarov, M.A. Koshelev, N.F. Zobov, O.V. Boyarkin, Chem. Phys. Lett. 627 (2015) 73.